Asian Journal of Chemistry; Vol. 35, No. 8 (2023), 1969-1978

ASIAN JOURNAL OF CHEMISTRY

https://doi.org/10.14233/ajchem.2023.28076

DFT, NBO, Fukui Functions and Monte Carlo Studies on Quinoline Derivatives for Corrosion Inhibition Property

A. CHARLES*, C. GOPI, P. ADWIN JOSE and S. PONSADAILAKSHMI

Department of Chemistry, E.G.S. Pillay Engineering College, Nagapattinam-611002, India

*Corresponding author: E-mail: charlesjoel408@gmail.com

Received: 21 May 2023; *Accepted*: 12 July 2023; *Published online*: 31 July 2023; AJC-21333

The corrosion inhibiting property of 4-methylquinoline (4MQ) and 4-aminoquinaldine (4A2MQ) by using various quantum mechanical and molecular mechanics parameters such as E_{HOMO}, E_{LUMO}, energy difference (ΔE_{gap}), electrophilicity, nucleophilicity, chemical hardness, chemical softness, adsorption energy on the metal surface, ability of back donation, electron affinity, chemical potential and dipole moment values are studied. Density functional studies were carried out using B3LYP/6-31g++(d,p), B3LYP/6-31g(d,p) and B3LYP/6-31g(d) basis sets. The outputs of the compounds were compared as well as the characteristics of the Fukui functions used to analyze them. The adsorption energy values were obtained using Monte Carlo simulation techniques. The adsorption energy calculations were carried out by using COMPASS force field and adsorption annealing methods. These calculated values had good agreement with previously reported values of these corrosion inhibitors. Comparing the combined dual descriptor values of 4MQ and 4A2MQ reveal that the latter compound readily undergoes electrophilic attack, leading to the enhanced corrosion inhibition. The efficiency of these corrosion inhibitors compounds by various studies was compared and the result shows that 4A2MQ can be better corrosion inhibitor than 4MQ.

Keywords: Quinoline derivatives, DFT, Fukui functions Monte Carlo simulation, Corrosion studies.

INTRODUCTION

Carbon steels appliances and machines play an important role in majority of the industries and day today life utilities. Protecting these materials from corrosion is very essential. Computational analysis of corrosion inhibitors has recently gained popularity among the scientists [1,2]. It is crucial to choose among the many reported organic based inhibitors based on their effectiveness and cost [3]. However, the microscopic mechanism of quinoline derivatives has not been investigated in spite of extensive experimental research. Different studies have shown that two quinoline derivatives *viz*. 4-methylquinoline (4MQ) and 4-aminoquinaldine (4A2MQ) worked as effective inhibitors but in different conditions [4,5]. To correlate and compare their efficiency general methodology need to be performed. Herein, we use the Monte Carlo approach and density functional theory (DFT) to conduct a thorough examination of inhibition efficiency and obtain accurate results in a simulated environment. This approach can be quite helpful in establishing the characteristics of each inhibitor and contrasting them to determine the superiority. The proximity of the inhibitor molecule to the metal controls its effectiveness as an inhibitor. The inhibitor is aligned flat, so that it covers as much of the metal as possible. The metropolis Monte Carlo method not only provides a visual representation of this direction, but it also allows for the numerical calculation of the energy liberated throughout the adsorption process [6]. Generally, adsorption is exothermic process and so the heat is evolved from the process. The total energy can be computed using the Monte Carlo method by adding deformation to the energy (E_{def}), rigid adsorption energy (E_{rigid}) and the inhibitor molecule energy [7-9].

$$E_{total} = E_{inhibitor} + E_{def} + E_{rigid}$$

The rigid adsorption energy (E_{rigid}) is the energy released during unrelaxed inhibitors molecule adsorbed by metal. On the other hand, E_{def} can be described as the energy released during the relaxed inhibitors molecules adsorbed by the metal. The negative value of the adsorption energy gives interaction energy (E_{int}) of the molecule [7-13].

$$E_{int} = E_{abs}$$

If the amount of interaction energy increases, there will be close binding possibilities between inhibitors and the metal. In turn, it gives greater amount of binding energy released during the interaction.

$$E_{bining} = E_{int}$$

Dudukcu & Avcl [4] reported that 4-aminoquinaldine (4A2MQ) as a competent inhibitor for mild steel impairment protection and evaluated the measurements of polarization resistance, electrochemical impedance spectroscopy (EIS) and potentiodynamic polarization only. However, the authors did not conduct the computational studies to comprehend the corrosion process at the microscopic levels. Similarly, Huang *et al.* [5] reported the corrosion inhibition of 4-methylquinoline (4MQ) and limited their work to weight loss method, surface analysis *via* SEM and electrochemical methods only. To interpret the surface analysis through other parameters such as adsorption energy, 4MQ become another compound of interest.

Therefore, the main focus of this study is on the quantum mechanical features of 4-aminoquinaldine (4A2MQ) and 4-methylquinoline (4MQ). The present work deals with the frontier molecular orbital analysis, natural bonding orbital analysis, Fukui functions analysis and metropolis Monte Carlo simulations analysis in order to explain the corrosion inhibitor property of two quinoline derivatives *viz*. 4-methylquinoline (4MQ) and 4-aminoquinaldine (4A2MQ).

EXPERIMENTAL

Quantum chemical calculations: The inhibitors molecules were optimized utilizing Gaussian 09 software suite [14]. The optimization process was carried out using B3LYP Becke three parameter [15] with Lee-Yang-Parr exchange correlation functional [16], 6-31g++(d,p), 6-31g(d,p), 6-31g(d) [17-19] and the basis sets were used. For the purpose of optimization process, the input files prepared using Gauss view 6.0 Software [20]. From the software the input files directly sent to optimization process.

Basis sets: The Basis sets 6-31g is split valence double zeta basis set. Alone "d" in the bracket means polarizing functions is applying to all heavy atoms. The function (d,p) means the first function for all heavy atoms and the second one for hydrogen atoms. These polarizing functions are used to study the properties like chemical bonding. The sign "+" and "++" is used to study compounds like ions and long range interactions. The diffuse functions "+" is used when the diffuse functions applied to heavy atoms. If the diffuse functions is applied to all atoms then the functions "++" have to be used [17-19]. Since 6-31g++(d,p) basis set contains polarize and diffuse functions, this basis set calculations were concentrated for further steps.

After optimization process, the single point energy calculations of the optimized structure were performed. During this calculations "save NBO" option also added. The output files were used to find HOMO, LUMO structures and ESP diagrams.

Condensed Fukui functions: The optimized structures of inhibitors obtained from DFT geometry optimization by basis sets 6-31g++(d,p) were the inputs of Multiwfn software [21]. This software initially generated three Gaussian Input files namely N.gif, N+1.gjf and N-1.gjf. Using this files population analysis calculated separately and wfn files obtained as output. The wfn files then set as input to the calculation of Fukui functions and condensed Fukui functions analysis.

Using Multiwfn software grid calculation was performed initially and then condensed Fukui functions has been calculated. The cube files generated during this processed to analyze Fukui Functions. The output CDFT.txt file used to interpret the condensed Fukui functions and condensed dual descriptors.

Adsorption energy calculations: To acquire the adsorption action of the inhibitors on the boundary of the iron metal surface material studio software has been used [22]. First the inhibitors molecules (4MQ and 4A2MQ) and water molecule were optimized using Forcite module using COMPASS force field. The Fe metal was then loaded from the structure gallery and cleaved as Fe(110) because it was reported as stable Fe stage with fair atomic density. The cleaved surface was used to make 11 × 11 super cell. After that vacuum slap was build at 40 Å thickness. By periodic boundary conditions, the generated simulation box at (27.306127 × 27.306127 × 50.134254) was used to find adsorption energy details by adsorption locator module.

By simulated annealing technique using COMPASS force field this metropolis Monte Carlo process was performed. For electrostic summation method, Ewald and group method (1.0×10^{-5} Kcal/mol) has applied and for van der Waals summation, atom based (Cutoff distance 1.85 nm) has applied. The minimum adsorption distance was set to 5 Å. The top layer of the Fe(1 1 0) was set as target atoms. This process was carried out 10 cycle and 100000 steps for each cycle to obtain fine quality.

Generally, the corrosion occurs in the presence of water. So the evaluation of adsorption behaviour in the presence of water molecules is also important. By using same experimental setup the same process repeated with 50 molecules of water as co-absorbate to 4MQ and 4A2MQ separately. The outputs Etotal.xcd, Fe(1 1 0).std, Fe(1 1 0)Fields.xsd, Fe(1 1 0).txt files were collected to analyze the field and absorption energy calculations.

RESULTS AND DISCUSSION

Geometry optimization: The geometry optimized structures of both inhibitors (4A2MQ and 4MQ) were obtained and investigated for the negative frequency. No such type of negative frequency vibrations present in the optimized structure. This indicates the particular structure is more stable with lower energy. Optimized structures are shown in Fig. 1 while the IR spectra is shown in Fig. 2.

Frontier molecular orbital analysis: In Table-1, the HOMO, LUMO, the energy gap between HOMO and LUMO, ionization potential, electron affinity, electronegativity, chemical potential, global harness, global softness, nucleophilicity, electrophilicity and back donation values are listed.

Energy gap: High value of HOMO denotes high ability of electron donating. A good inhibitor can donate electron to the metal surface. Similarly, low value of LUMO is also an important property for good inhibitor. High difference between HOMO and LUMO indicates that the molecule is the stable

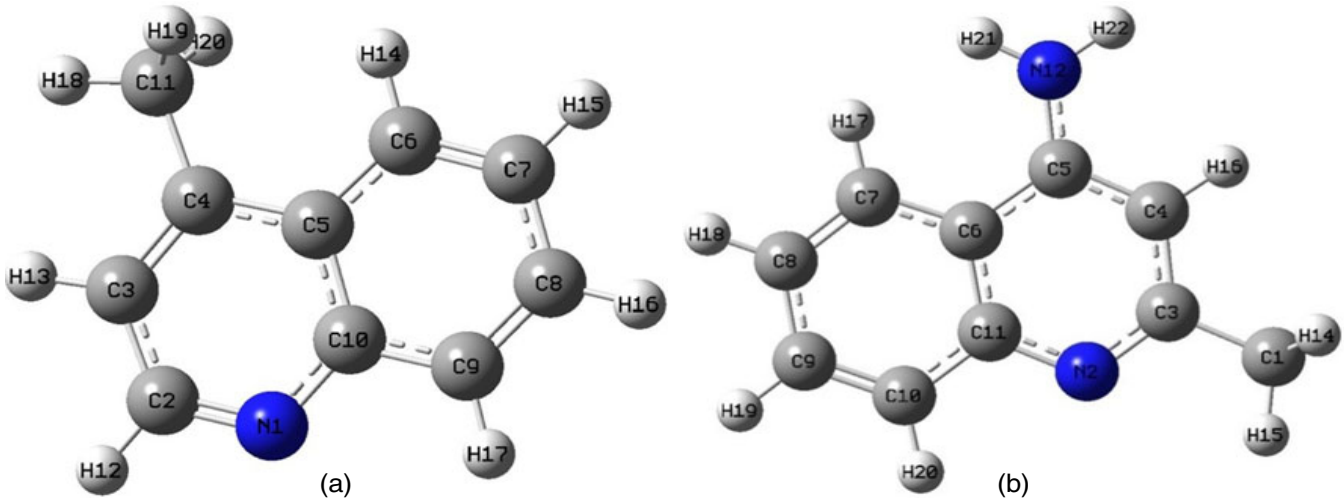

Fig. 1. Optimized structure of the inhibitor (a) 4MQ, (b) 4A2MQ

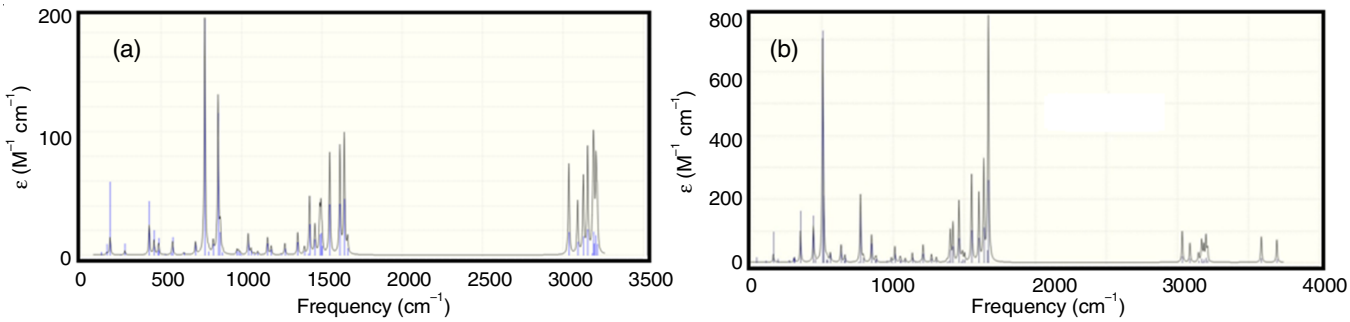

Fig. 2. Vibrational spectra of (a) 4MQ and (b) 4A2MQ obtained from 631g++(d,p) basis sets

TABLE-1
VARIOUS QUANTUM CHEMICAL PARAMETERS FOR 4-METHYLQUINOLINE (4MQ) AND 4-AMINOQUINALDINE (4A2MQ)

Property	Basis sets					
	6-31g++(d,p)		6-31g(d,p)		6-31g(d)	
	4MQ	4A2MQ	4MQ	4A2MQ	4MQ	4A2MQ
E_{HOMO}	-6.4733	-5.9305	619495	562079	618678	562215
E_{LUMO}	-1.6958	-1.3233	132329	90369	131132	89906
ΔE_{gap}	4.77751	4.60716	4871657	4717096	487547	472308
Ionization potential	6.47332	5.93045	619495	5620787	6186784	5622147
Electron affinity	1.69581	1.32329	132329	90369	131132	89907
Electronegativity	4.08457	3.62687	375912	326224	374905	326061
Chemical potential	-4.0845	-3.6269	375912	326224	374905	326061
Global hardness	2.38875	2.30358	243583	235855	243773	236154
Global softness	0.41863	0.43411	41054	42399	41022	42345
Electrophilicity	3.49213	2.85516	290065	225609	288288	225098
Nucleophilicity	0.28636	0.35024	34475	44324	34688	44425
ΔN	0.61024	0.73215	0.66525	0.79239	0.6668	0.79173
Back donation	-0.5972	-0.5759	–060896	–058964	–060943	–059039

one (Fig. 3) [22]. For 4MQ, the energy difference is 4.77751 eV and for 4A2MQ the value is 4.6071eV. In comparison to 4MQ, 4A2MQ is a more potent inhibitor because its HOMO-LUMO energy gap is smaller. It should also be pointed out that the energy gap of 4MQ is significantly lower than that of the previously reported quinoline derivatives inhibitors [23,24].

Electronegativity and chemical potential: A beneficial anticorrosive substance shows minimum electronegativity amount. Results shown in Table-1 indicates that 4A2MQ can be a good inhibitor since its electronegativity value is higher than that of 4MQ [25]. The chemical potential is a negative value of electronegativity. Therefore, it is reasonable to predict the same inhibitory efficiency regardless of the chemical potential value.

Electrophilicity and nucleophilicity: Inhibitors 4MQ and 4A2MQ differ in electrophilicity, with 4MQ having a higher value. The nucleophilicity value of 4A2MQ is quite high, since they may donate more electrons.

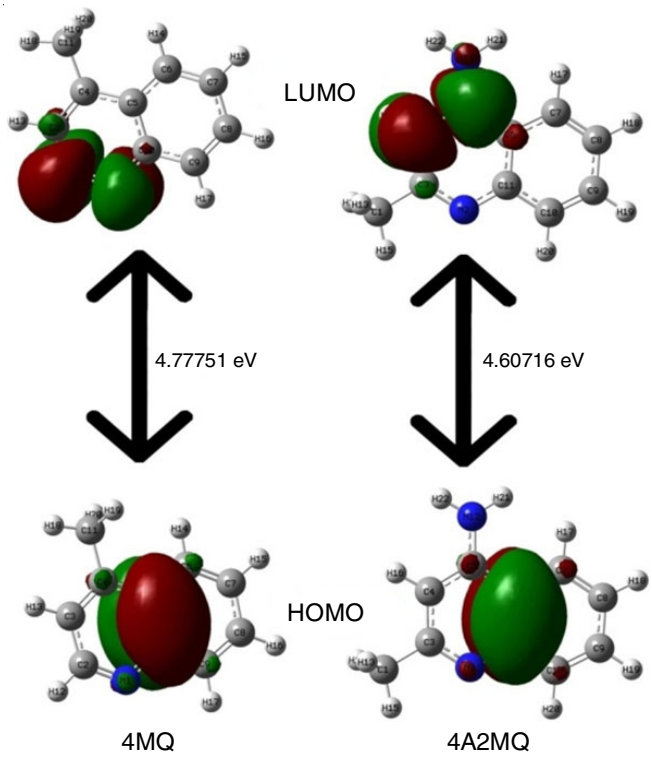

Fig. 3. FMO of the corrosion inhibitors by using DFT at B3LYP/6-31G

Global hardness and global softness: Global hardness and global softness are the indices of chemical vulnerability. For a good inhibitor molecule the global softness value should below and global softness value should be high [26]. In Table-1, the order of chemical hardness is 4MQ > 4A2MQ and the order of global softness is 4A2MQ > 4MQ. This indicates 4A2MQ is the best inhibitor from the concerned two compounds.

Energy of back donation: If global hardness value is greater than zero, the value of $\Delta E_{back\ donation}$ is also less than zero. This situation energetically favours the back giving from molecule to the surface of the metal. From Table-1 as expected, the calculated $\Delta E_{back\ donation}$ values exhibits the tendency 4A2MQ > 4MQ.

Dipole moments and polarizability: The non-uniform distribution of charges of atom in a molecule leads to the polarization of covalent bonds. This quantity can be measured as dipole moments. High value of dipole moments favours the interaction between inhibitor and metal [24]. Results (Table-2) show that the dipole moment of 4A2MQ is greater than 4MQ, so, it can have better physical phenomenon with metal surface. Similarly, the polarizability results also show same conclusion.

Fractions of electron transferred: According to Lukovits *et al.* [23], if $\Delta N < 0$ the corrosion resisting kill fullness of the molecule was increases. From Table-1, the ΔN value is less than 3.6 for both inhibitors, which indicated that both inhibitor molecules have high tendency to give electron to the metal surface. Out of these two inhibitors 4MQ and 4A2MQ, the Δ value of 4A2MQ is greater than 4MQ, which clearly tells that 4A2MQ has high ability of electron donating efficiency than 4MQ, hence it can acts as a good inhibitor.

Molecular electrostatic potential (MEP): Molecular electrostatic potential (MEP) is a useful tool to identify the reactive site in a molecule. Different colours represent the different electrostatic potential value [27-30]. Fig. 4 shows the MEP structure of 4MQ and 4A2MQ. The red areas denote

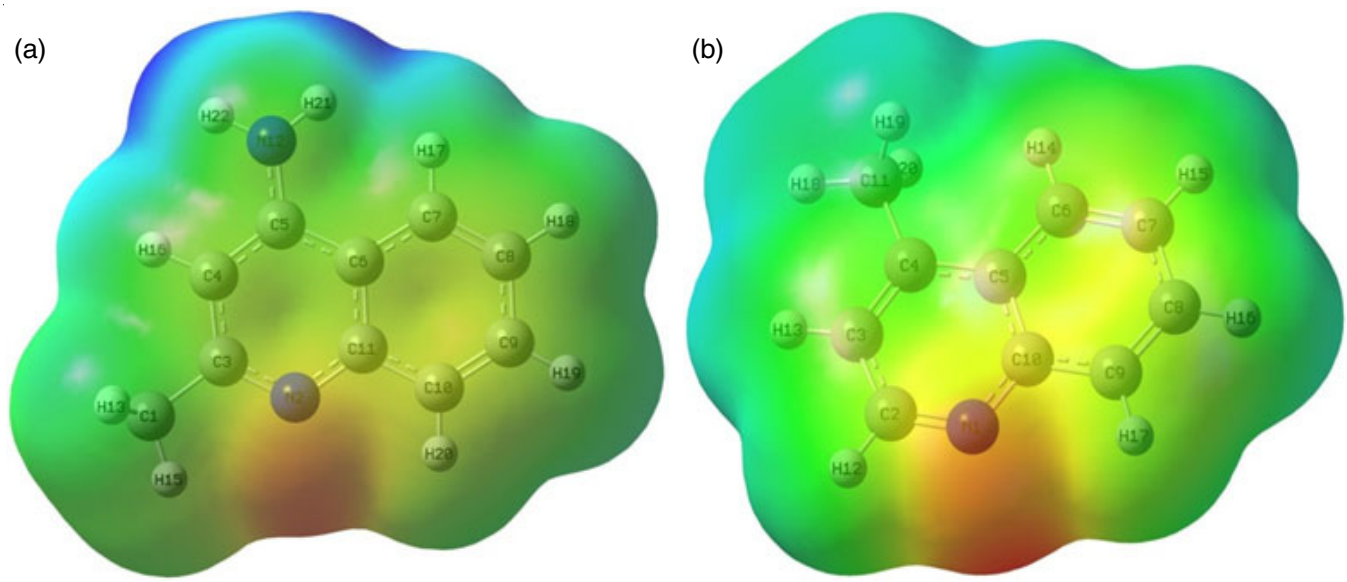

Fig. 4. MEP structure of (a) 4-methylquinoline (4MQ) and (b) 4-aminoquinaldine (4A2MQ)

TABLE-2
DIPOLE MOMENT AND POLARIZABILITY VALUES

	Dipole moment (Debye)			Polarizability (a.u.)		
	6-31g++(d,p)	6-31g(d,p)	6-31g(d)	6-31g++(d,p)	6-31g(d,p)	6-31g(d)
4-Methylquinoline (4MQ)	2.66008	2.45464	2.44251	124.64433	107.12833	106.38133
4-Aminoquinaldine (4A2MQ)	3.46597	3.41049	3.39646	138.07000	118.18767	117.39300

those that can be attacked by an electrophile, whereas the blue areas can be attacked by a nucleophile. The order of colour with respect to potential is in the order of red < orange < yellow < green < blue [29]. So red, orange and yellow colour region can donate the electrons to metal surface.

Reactive site analysis

4-Methylquinoline (4MQ): The condensed Fukui functions indices values obtained from the multi.wfn for 4MQ inhibitor are listed in Table-3 and the outcome of these values are plotted in Fig. 5, whereas Fig. 6 shows the nucleophilicity and electrophilicity of each atom present in the molecule. Fig. 7 reveals the condensed dual descriptors of atoms present in the 4MQ inhibitor molecule. From Fig. 6, it was concluded that most of the atoms present in the 4MQ molecule act as nucleophiles. As compared to electrophilicity, the amount of nucleophilicity displayed by (N1), (C6), and (C9) is particularly significant and these results are consistent with the HOMO and LUMO plots.

The condensed dual descriptors values of atoms (C6) and (C9) give the same results with condensed Fukui functions. These molecules have a preference for negatively charged atoms because electrophiles are attracted to negatively charged atoms. Even though (N1) shows high nucleophilicity, its CDD value is positive but too small compare with other atoms. As a result, the most likely sites of electrophile attack are (C6) and (C9). The softness values, relative electrophilicity and nucleophilicity values of (C6) and (C9) in Table-4 are comparatively different with other values present in the same molecules.

4-Aminoquinaldine (4A2MQ): The condensed Fukui and condensed dual descriptors values are given in Table-5 and their graphical plots are represented in Figs. 8-10. In 4A2MQ

TABLE-3
CONDENSED FUKUI FUNCTIONS PARAMETERS OF 4-METHYLQUINOLINE (4MQ)

Atom	f–	f+	f0	CDD	Electrophilicity	Nucleophilicity
N1	0.0804	0.0833	0.0819	0.0029	0.08718	0.21298
C2	0.0592	0.0820	0.0706	0.0228	0.08580	0.15665
C3	0.0710	0.0651	0.0680	-0.0059	0.06806	0.18794
C4	0.0630	0.0760	0.0695	0.01300	0.0795	0.16694
C5	0.0140	0.0146	0.0143	0.0006	0.01528	0.03714
C6	0.1036	0.0672	0.0854	-0.0365	0.07029	0.27445
C7	0.0736	0.0657	0.0696	-0.0079	0.06875	0.19486
C8	0.0688	0.0627	0.0658	-0.0061	0.06563	0.18220
C9	0.1062	0.0723	0.0892	-0.0339	0.07562	0.28124
C10	0.0204	0.0181	0.0192	-0.0023	0.01892	0.05390
C11	0.0186	0.0235	0.0211	0.0048	0.02454	0.04938
H12	0.0386	0.0511	0.0449	0.0126	0.05350	0.10218
H13	0.0385	0.0463	0.0424	0.0078	0.04844	0.10206
H14	0.0405	0.0377	0.0391	-0.0029	0.03940	0.10734
H15	0.0420	0.0427	0.0424	0.0007	0.04473	0.11128
H16	0.0414	0.0423	0.0419	0.0009	0.04429	0.10971
H17	0.0449	0.0421	0.0435	-0.0028	0.04405	0.11901
H18	0.0245	0.0265	0.0255	0.0020	0.02774	0.06498
H19	0.0250	0.0383	0.0316	0.0133	0.04002	0.06613
H20	0.0250	0.0382	0.0316	0.0133	0.04002	0.06612

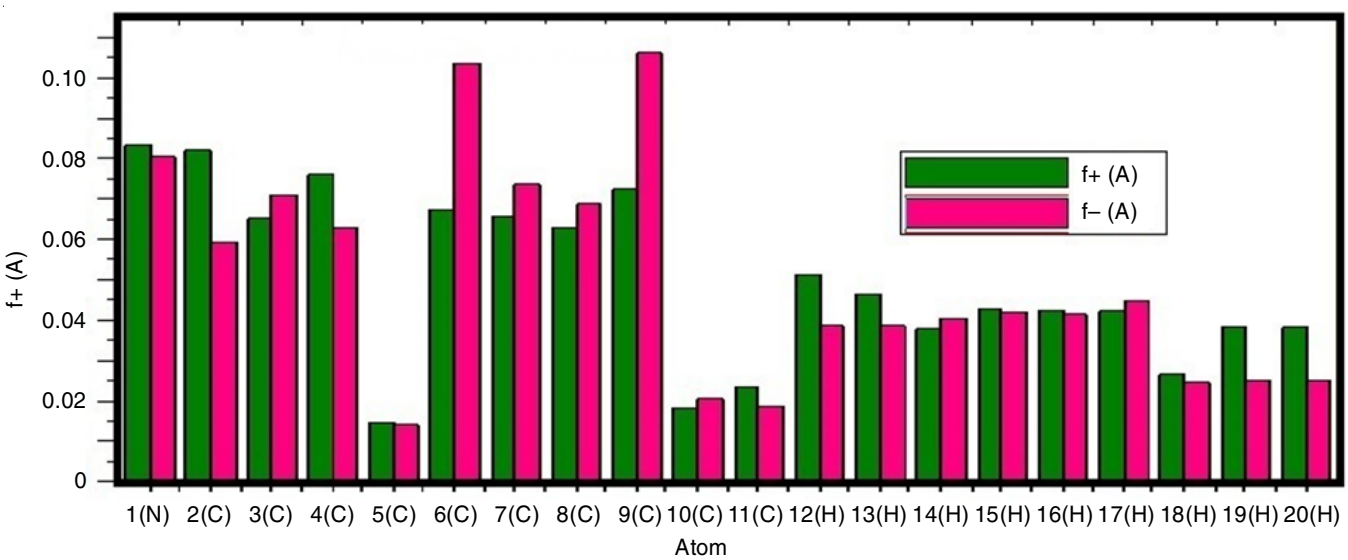

Fig. 5. Condensed Fukui functions value of 4-methylquinoline (4MQ)

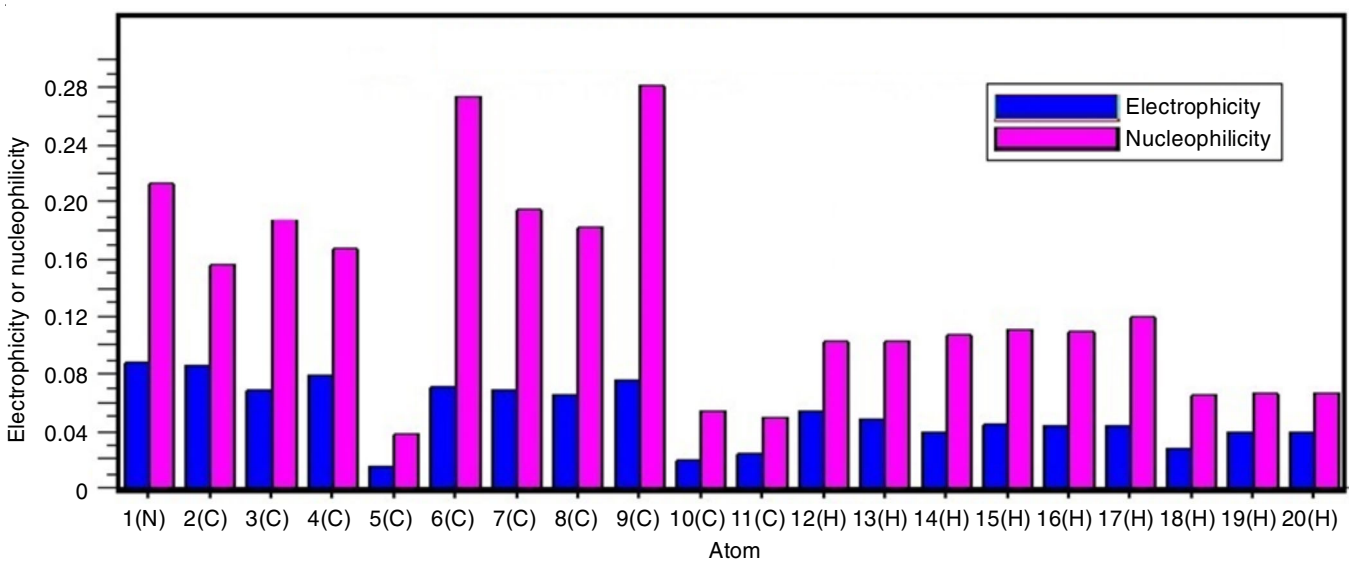

Fig. 6. Electrophicity and nucleophilicity of each atom in 4-methylquinoline (4MQ) inhibitor

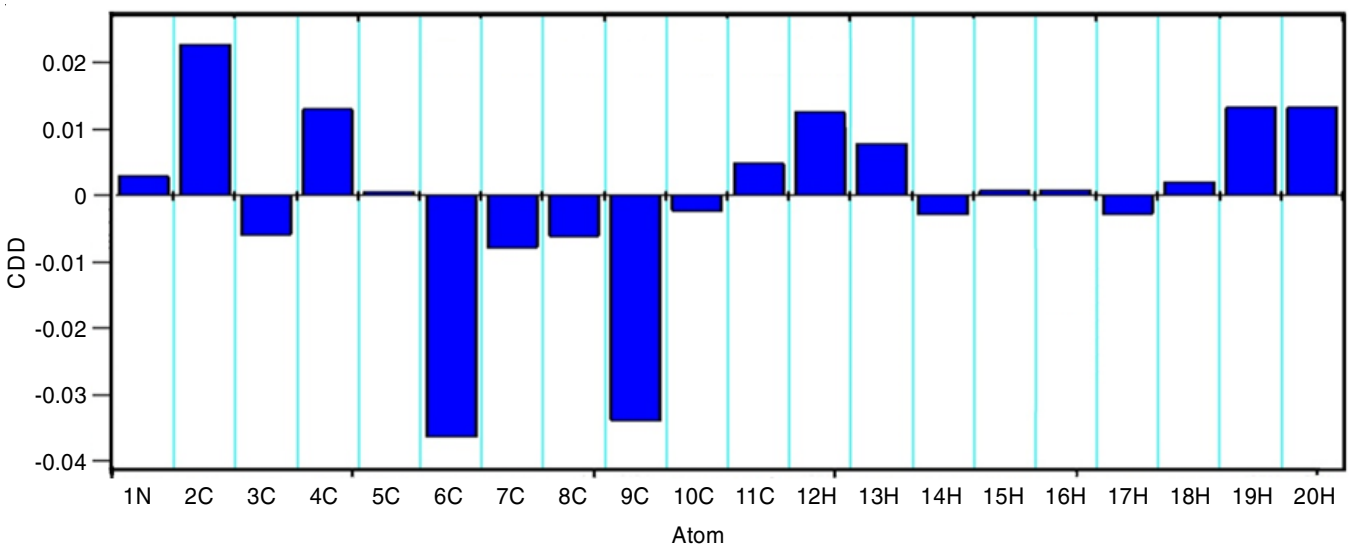

Fig. 7. Condensed dual descriptors of 4-methylquinoline (4MQ)

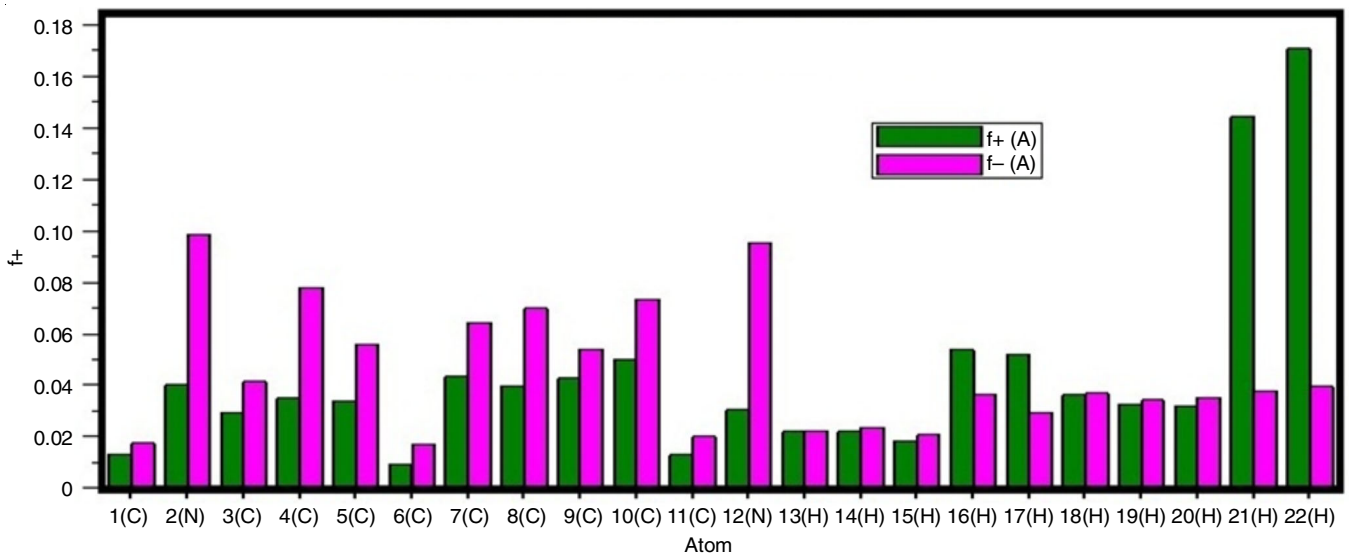

Fig. 8. Condensed Fukui functions values of 4-aminoquinaldine (4A2MQ)

TABLE-4
CONDENSED LOCAL SOFTNESSES (Hartree*e) AND RELATIVE ELECTROPHILICITY/NUCLEOPHILICITY (DIMENSIONLESS) FOR 4MQ

Atom	s–	s+	s0	s+/s–	s–/s+
1(N)	0.2654	0.2749	0.2702	1.0359	0.9653
2(C)	0.1952	0.2706	0.2329	1.3861	0.7214
3(C)	0.2342	0.2146	0.2244	0.9165	1.0911
4(C)	0.2080	0.2508	0.2294	1.2055	0.8295
5(C)	0.0463	0.0482	0.0472	1.0415	0.9601
6(C)	0.3420	0.2217	0.2818	0.6482	1.5426
7(C)	0.2428	0.2168	0.2298	0.8929	1.1199
8(C)	0.2270	0.2070	0.2170	0.9117	1.0969
9(C)	0.3504	0.2385	0.2945	0.6805	1.4695
10(C)	0.0672	0.0597	0.0634	0.8886	1.1254
11(C)	0.0615	0.0774	0.0695	1.2579	0.7950
12(H)	0.1273	0.1687	0.1480	1.3253	0.7546
13(H)	0.1272	0.1528	0.1400	1.2012	0.8325
14(H)	0.1337	0.1242	0.1290	0.9289	1.0765
15(H)	0.1387	0.1410	0.1399	1.0172	0.9831
16(H)	0.1367	0.1397	0.1382	1.0218	0.9787
17(H)	0.1483	0.1389	0.1436	0.9369	1.0674
18(H)	0.0810	0.0875	0.0842	1.0806	0.9254
19(H)	0.0824	0.1262	0.1043	1.5317	0.6529
20(H)	0.0824	0.1262	0.1043	1.5317	0.6529

inhibitor molecule (N2), (N12) and atoms have high f– values. Sites with high nucleophilicity are good targets for electrophilic attack since they are willing to donate the electrons to the metal surface. These results were compared and agreed with the relative electrophilicity and nucleoophicity values as shown in Table-5.

The condensed dual descriptors value of 4A2MQ are plotted in Fig. 10, which shows that atoms (N2), (N12), (C4), (C5), (C7), (C8), (C10) have negative values. These results indicates these atoms are favourable for electrophilic attack. Hydrogen 21 and 22 only have high value of positive CDD. Similarly in Table-6, the (N2), (N12), (C4), (C5), (C7), (C8), (C10) values are different with other atoms present in the inhibitor molecule.

TABLE-6
CONDENSED LOCAL SOFTNESSES (Hartreee) AND RELATIVE ELECTROPHILICITY/NUCLEOPHILICITY (DIMENSIONLESS) FOR 4A2MQ

Atom	s–	s+	s0	s+/s–	s–/s+
1(C)	0.0697	0.0532	0.0614	0.7639	1.3091
2(N)	0.3936	0.1603	0.2769	0.4072	2.4556
3(C)	0.1655	0.1179	0.1417	0.7125	1.4036
4(C)	0.3115	0.1397	0.2256	0.4484	2.2302
5(C)	0.2238	0.1359	0.1798	0.6072	1.6468
6(C)	0.0678	0.0363	0.0521	0.5352	1.8685
7(C)	0.2575	0.1736	0.2156	0.6741	1.4835
8(C)	0.2794	0.1588	0.2191	0.5685	1.7589
9(C)	0.2157	0.1703	0.1930	0.7894	1.2667
10(C)	0.2930	0.2012	0.2471	0.6866	1.4564
11(C)	0.0798	0.0521	0.0659	0.6528	1.5319
12(N)	0.3819	0.1215	0.2517	0.3181	3.1439
13(H)	0.0896	0.0876	0.0886	0.9775	1.0230
14(H)	0.0941	0.0882	0.0911	0.9366	1.0677
15(H)	0.0826	0.0735	0.0781	0.8898	1.1239
16(H)	0.1464	0.2152	0.1808	1.4698	0.6804
17(H)	0.1170	0.2083	0.1627	1.7801	0.5618
18(H)	0.1473	0.1449	0.1461	0.9837	1.0165
19(H)	0.1367	0.1309	0.1338	0.9571	1.0448
20(H)	0.1407	0.1270	0.1339	0.9023	1.1083
21(H)	0.1510	0.5777	0.3644	3.8247	0.2615
22(H)	0.1574	0.6841	0.4207	4.3471	0.2300

Monte Carlo simulations: Figs. 11 and 12 show the equilibrium adsorption configurations. In these simulations carbon atoms represented by light black balls. Hydrogen atoms represented by white balls. Water molecules is shown in wire model. Dark blue colour represents nitrogen atom. In the surface plane the balls surrounded by orange lines are the target atoms for these simulations. Flat alignment of the organic inhibitor compound towards the mild steel boundary covers maximum area. So flat orientation favours maximum inhibition performance. From Fig. 12, it is found that flat orientation of both inhibitors would give the maximum inhibition efficiency.

TABLE-5
CONDENSED FUKUI FUNCTIONS PARAMETERS OF 4-AMINOQUINALDINE (4A2MQ)

Atom	f–	f+	f0	CDD	Electrophilicity	Nucleophilicity
C1	0.0174	0.0133	0.0153	-0.0041	0.01379	0.05574
N2	0.0983	0.0400	0.0692	-0.0583	0.04152	0.31489
C3	0.0413	0.0295	0.0354	-0.0119	0.03055	0.13244
C4	0.0778	0.0349	0.0563	-0.0429	0.03618	0.24923
C5	0.0559	0.0339	0.0449	-0.0219	0.03520	0.17902
C6	0.0169	0.0091	0.0130	-0.0079	0.00940	0.05425
C7	0.0643	0.0434	0.0538	-0.0210	0.04497	0.20604
C8	0.0698	0.0397	0.0547	-0.0301	0.04115	0.22352
C9	0.0539	0.0425	0.0482	-0.0113	0.04412	0.17261
C10	0.0732	0.0502	0.0617	-0.0229	0.05212	0.23442
C11	0.0199	0.0130	0.0165	-0.0069	0.01349	0.06384
N12	0.0954	0.0303	0.0629	-0.0650	0.03147	0.30557
H13	0.0224	0.0219	0.0221	-0.0005	0.02269	0.07170
H14	0.0235	0.0220	0.0228	-0.0015	0.02284	0.07530
H15	0.0206	0.0184	0.0195	-0.0023	0.01905	0.06611
H16	0.0366	0.0537	0.0452	0.0172	0.05575	0.11714
H17	0.0292	0.0520	0.0406	0.0228	0.05397	0.09363
H18	0.0368	0.0362	0.0365	-0.0006	0.03753	0.11784
H19	0.0341	0.0327	0.0334	-0.0015	0.03390	0.10939
H20	0.0351	0.0317	0.0334	-0.0034	0.03290	0.11260
H21	0.0377	0.1443	0.0910	0.1066	0.14965	0.12084
H22	0.0393	0.1708	0.1051	0.1315	0.17722	0.12591

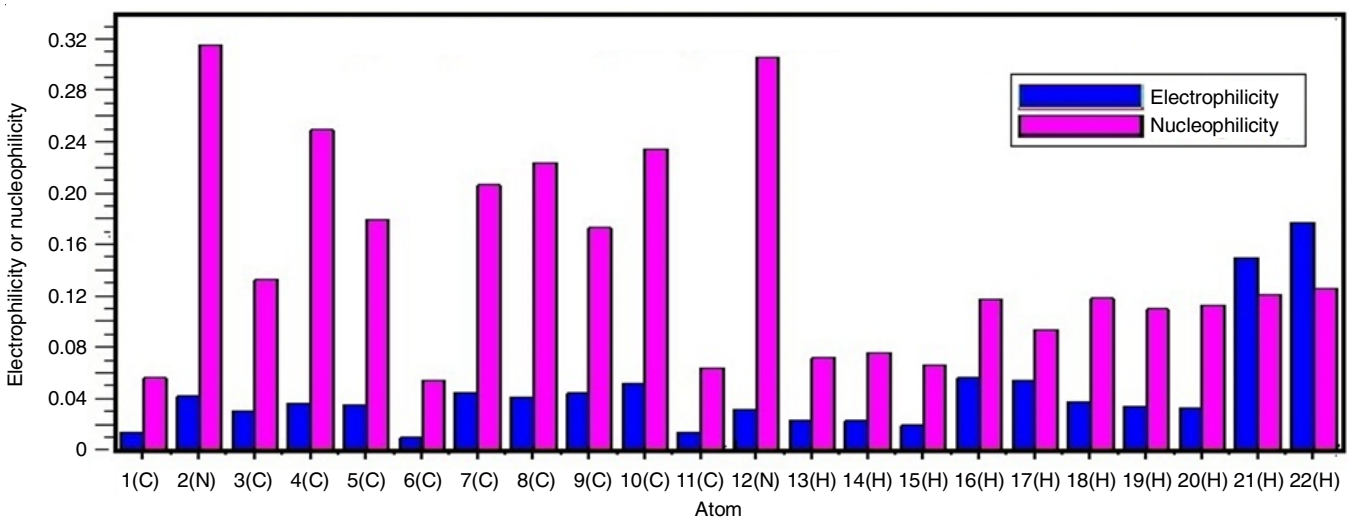

Fig. 9. Electrophilicity and nucleophilicity of each atom in 4-aminoquinaldine (4A2MQ) inhibitor

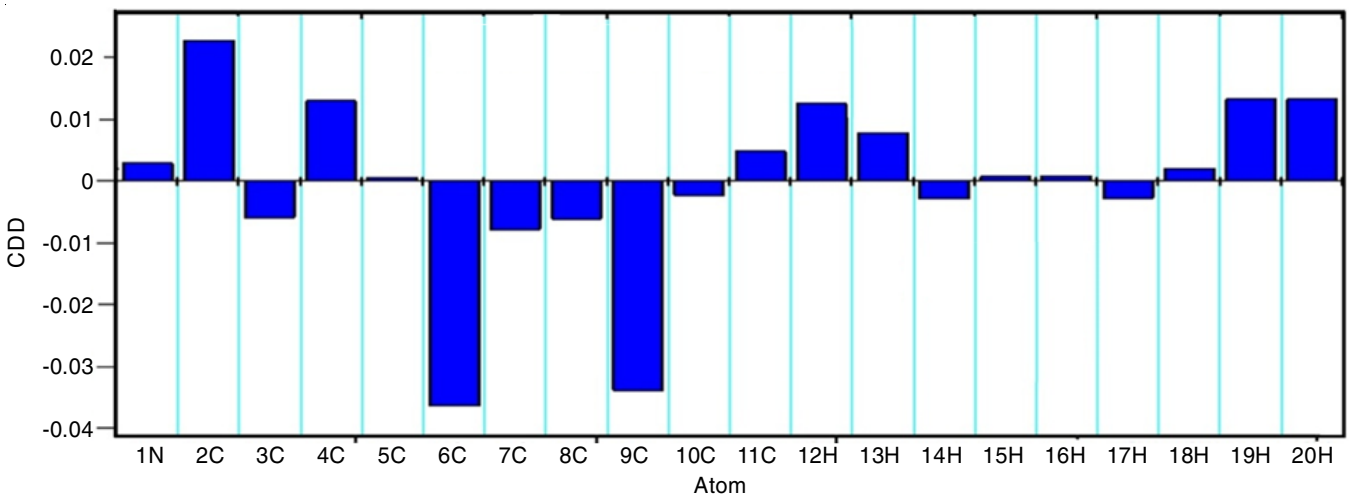

Fig. 10. Condensed dual descriptors of 4-aminoquinaldine (4A2MQ)

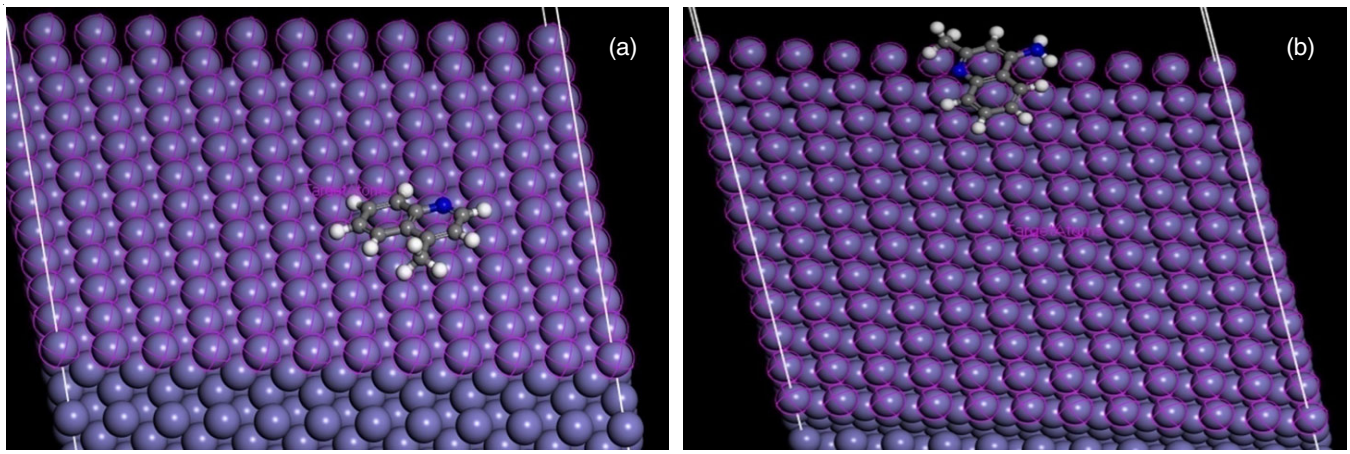

Fig. 11. Equilibrium adsorption configurations of (a) 4MQ/Fe(110) and (b) 4A2MQ/Fe(110)

Both inhibitors have high negative values of adsorption energy. The greater negative value of adsorption energy indicates the inhibition power. The adsorption energy produced by Monte Carlo simulation techniques are presented in Table-7, and it is concluded that the adsorption energy of 4A2MQ is greater than that of 4MQ. So out of these two compounds 4A2MQ is more efficient than 4MQ.

Fig. 13 represent the total energy profile for the equilibrium adsorption configurations of 4MQ and 4A2MQ on the metal surface without any other co-adsorbents.When water

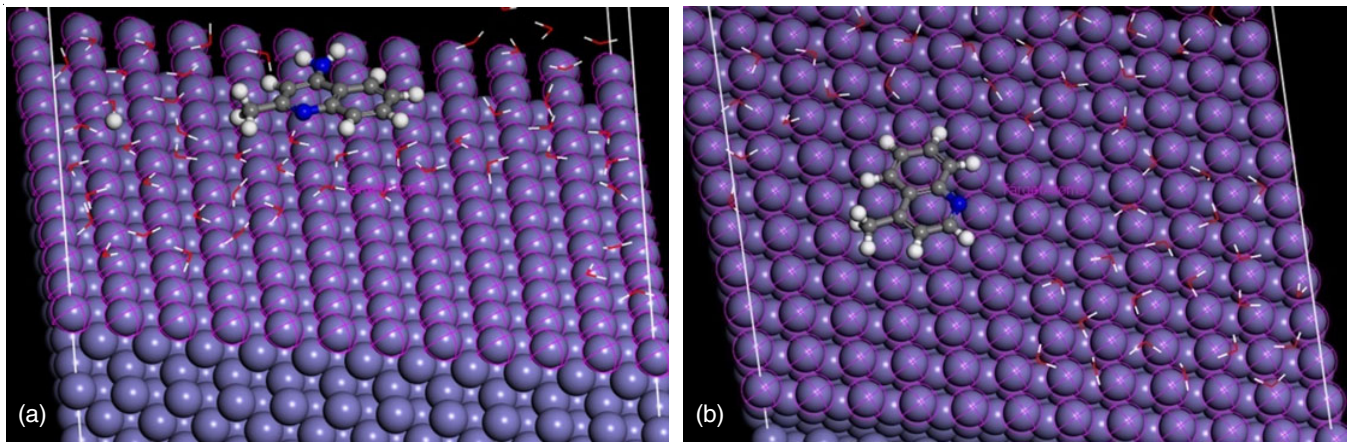

Fig. 12. Equilibrium adsorption configurations of (a) 4MQ/Fe(110)/50H_2O and (b) 4A2MQ/Fe(110)/50H_2O

TABLE-7
ADSORPTION ENERGIES FOR THE EQUILIBRIUM ADSORPTION CONFIGURATIONS OF 4-METHYLQUINOLINE (4MQ) AND 4-AMINOQUINALDINE (4A2MQ) MOLECULES IN THE ABSENCE OF WATER MOLECULES

Adsorption energy of 4-methylquinoline (4MQ)					
Structures	Total energy	Adsorption energy	Rigid adsorption energy	Deformation energy	4MQ: dEad/dNi
Fe (110)	-28.44960	-88.45336116	-89.23505415	0.78169299	-88.45336
Adsorption energy of 4-aminoquinaldine (4A2MQ)					
Structures	Total energy	Adsorption energy	Rigid adsorption energy	Deformation energy	4A2MQ: dEad/dNi
Fe (110)	-58.660755	-96.90182104	-97.37011289	0.468291849	-96.90182

Note: Units Kcal/mol

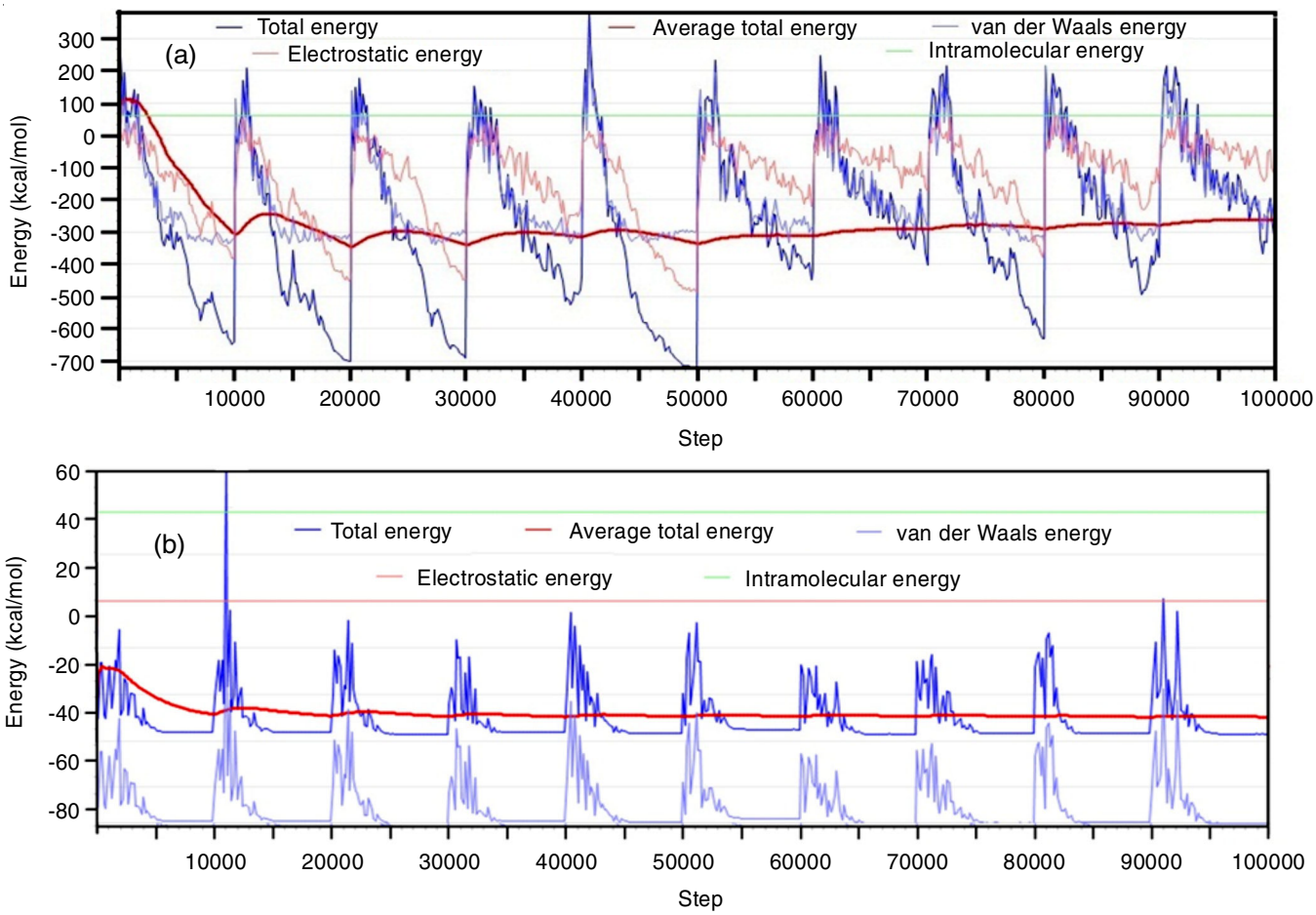

Fig. 13. Energy profile diagrams for the equilibrium adsorption configurations of (a) 4MQ/Fe(110) and (b) 4A2MQ/Fe(110)

TABLE-8
ADSORPTION ENERGIES FOR THE EQUILIBRIUM ADSORPTION CONFIGURATIONS OF 4-METHYLQUINOLINE (4MQ) AND 4-AMINOQUINALDINE (4A2MQ) MOLECULES IN THE PRESENCE OF WATER MOLECULES

Adsorption Energy of 4-aminoquinaldine (4A2MQ) in the presence of 50 water molecule						
Structures	Total energy	Adsorption energy	Rigid adsorption energy	Deformation energy	Water: dEad/dNi	4MQ: dEad/dNi
Fe (110)	-813.548	-873.552075	-908.972445	35.420369	-17.76701	-89.616
Adsorption energy of 4-aminoquinaldine (4A2MQ) in the presence of 50 water molecule						
Structures	Total energy	Adsorption energy	Rigid adsorption energy	Deformation energy	Water: dEad/dNi	4A2MQ: dEad/dNi
Fe (110)	-844.503	-882.744552	-917.085234	34.34068201	-17.74629	-108.899

Units: Kcal/mol

molecules are present, the same types of results are also observed. In Table-8, when compare the dE_{ad}/dNi value of water and 4MQ, the dE_{ad}/dN_i value of 4MQ is too high. The same trend observed in 4A2MQ inhibitors also. The results suggest that 4A2MQ as compared to 4MQ has a higher value of adsorption energy because of higher interaction energy.

Conclusion

In present work, two quinoline derivatives *viz*. 4-methylquinoline (4MQ) and 4-aminoquinaldine (4A2MQ) were optimized and their reactive sites were aslo analyzed through condensed Fukui functions parameters. Inhibitor interaction with metal surfaces were analyzed by Monte Carlo simulations techniques. Corrosion resistance efficiency of both inhibitors were compared by DFT, Fukui functions and adsorption energy parameters. The results indicated that 4A2MQ has high reactivity than 4MQ. Flat orientation of 4A2MQ and 4MQ gives the maximum inhibition efficiency due to the releases maximum amount of adsorption energy during interaction with metal surface. Electron donating, back donation efficiencies, dipole moment value, polarizability value, chemical potential values, nucleophilicity and electrophilicity values, Fukui indices and HOMO-LUMO energy gap values favours 4A2MQ better corrosion inhibitor than 4MQ.

CONFLICT OF INTEREST

The authors declare that there is no conflict of interests regarding the publication of this article.

REFERENCES

1. D.K. Verma, R. Aslam, J. Aslam, M.A. Quraishi, E.E. Ebenso and C. Verma, *J. Mol. Struct.*, **1236**, 130294 (2021); https://doi.org/10.1016/j.molstruc.2021.130294
2. F.E. Abeng, B.E. Nyong, M.E. Ikpi and M.E. Obeten, *Portug. Electrochim. Acta*, **40**, 243 (2022); https://doi.org/10.4152/pea.2022400402
3. L. Chen, D. Lu and Y. Zhang, *Materials*, **15**, 2023 (2022); https://doi.org/10.3390/ma15062023
4. M. Düdükcü and G. Avci, *Res. Chem. Intermed.*, **41**, 4861 (2015); https://doi.org/10.1007/s11164-014-1572-2
5. W. Huang, L. Hu, C. Liu, J. Pan, Y. Tian and K. Cao, *Int. J. Electrochem. Sci.*, **13**, 11273 (2018); https://doi.org/10.20964/2018.11.90
6. C. Verma, H. Lgaz, D.K. Verma, E.E. Ebenso, I. Bahadur and M.A. Quraishi, *J. Mol. Liq.*, **260**, 99 (2018); https://doi.org/10.1016/j.molliq.2018.03.045
7. J. Bartley, N. Huynh, S.E. Bottle, H. Flitt, D.P. Schweinsberg and T. Notoya, *Corros. Sci.*, **45**, 81 (2003); https://doi.org/10.1016/S0010-938X(02)00051-3
8. L. Guo, S.T. Zhang, T.M. Lv and W.J. Feng, *Res. Chem. Intermed.*, **41**, 3729 (2015); https://doi.org/10.1007/s11164-013-1485-5
9. L. Guo, C. Qi, X. Zheng, R. Zhang, X. Shen and S. Kaya, *RSC Adv.*, **7**, 29042 (2017); https://doi.org/10.1039/C7RA04120A
10. C. Verma, L.O. Olasunkanmi, E.E. Ebenso, M.A. Quraishi and I.B. Obot, *J. Phys. Chem. C*, **120**, 11598 (2016); https://doi.org/10.1021/acs.jpcc.6b04429
11. H. Shokry, *J. Mol. Struct.*, **1060**, 80 (2014); https://doi.org/10.1016/j.molstruc.2013.12.030
12. S.K. Saha, A. Dutta, P. Ghosh, D. Sukul and P. Banerjee, *Phys. Chem. Chem. Phys.*, **18**, 17898 (2016); https://doi.org/10.1039/C6CP01993E
13. H. Shokry and E.M. Mabrouk, *Arab. J. Chem.*, **10**, S3402 (2017); https://doi.org/10.1016/j.arabjc.2014.01.023
14. K. Zhou, R. Enos, D. Zhang and J. Tang, *Compos. Struct.*, **280**, 114816 (2022); https://doi.org/10.1016/j.compstruct.2021.114816
15. A.D. Becke, *J. Chem. Phys.*, **98**, 1372 (1993); https://doi.org/10.1063/1.464304
16. C. Lee, W. Yang and R.G. Parr, *Phys. Rev. B Condens. Matter*, **37**, 785 (1988); https://doi.org/10.1103/PhysRevB.37.785
17. T. Clark, J. Chandrasekhar, G.W. Spitznagel and P.V.R. Schleyer, *J. Comput. Chem.*, **4**, 294 (1983); https://doi.org/10.1002/jcc.540040303
18. P.C. Hariharan and J.A. Pople, *Theor. Chim. Acta*, **28**, 213 (1973); https://doi.org/10.1007/BF00533485
19. W.J. Hehre, R. Ditchfield and J.A. Pople, *J. Chem. Phys.*, **56**, 2257 (1972); https://doi.org/10.1063/1.1677527
20. D. Roy, T.A. Keith and J.M. Millam, Gauss View Version 6, Semichem Inc. Shawnee Mission KS (2019).
21. L. Tian and F. Chen, *J. Comput. Chem.*, **33**, 466 (2012); https://doi.org/10.1002/jcc.21992
22. D.S. Biovia, Materials Studio, R2 Dassault Systèmes BIOVIA, San Diego (2017).
23. I. Lukovits, E. Kalman and F. Zucchi, *Corrosion*, **57**, 3 (2001); https://doi.org/10.5006/1.3290328
24. L. Jiang, Y. Qiang, Z. Lei, J. Wang, Z. Qin and B. Xiang, *J. Mol. Liq.*, **255**, 53 (2018); https://doi.org/10.1016/j.molliq.2018.01.133
25. C.T. Ser, P. Zuvela and M.W. Wong, *Appl. Surf. Sci.*, **512**, 145612 (2020); https://doi.org/10.1016/j.apsusc.2020.145612
26. S.K. Saha, P. Ghosh, A. Hens, N.C. Murmu and P. Banerjee, *Physica E*, **66**, 332 (2015); https://doi.org/10.1016/j.physe.2014.10.035
27. P.-O. Lowdin, Advances in Quantum Chemistry, Academic Press (1979).
28. F.J. Luque, M. Orozco, P.K. Bhadane and S.R. Gadre, *J. Phys. Chem.*, **97**, 9380 (1993); https://doi.org/10.1021/j100139a021
29. P.C. Mishra and A. Kumar, Theoretical and Computational Chemistry, Book Series, Elsevier, vol. 3, p. 257 (1996); https://doi.org/10.1016/S1380-7323(96)80046-X
30. I. Alkorta and J.J. Perez, *Int. J. Quantum Chem.*, **57**, 123 (1996); https://doi.org/10.1002/(SICI)1097-461X(1996)57:1<123::AID-QUA14>3.0.CO;2-9